

Highly Wettable Slippery Surfaces: Self-cleaning Effect and Mechanism

K.Y. LAW*

Research and Innovative Solutions, 27 Valewood Run, Penfield, NY 14526, USA

Self-cleaning surface is usually superhydrophobic and non-wettable, characterized by a large static contact angle ($\geq 150^\circ$) and a small sliding angle ($\leq 10^\circ$). In contrast, wettable surfaces are surfaces with small static contact angles (e.g., $< 90^\circ$). It is very uncommon to have surfaces that are highly wettable and slippery (sliding angles $\leq 10^\circ$) at the same time. In this report, recent work on wettable, slippery surfaces are reviewed. Results show that the key enabler for self-cleaning is surface slipperiness, not the large static contact angle as many suggested. Further investigation reveals that the main contributor to surface slipperiness is the small contact angle hysteresis. Structure-property relationship studies of many wettable slippery surfaces suggest that fast molecular relaxation occurs during advancing at the liquid-solid interface, which leads to comparable advancing and receding angle and consequently small hysteresis. Additional supporting data for this interpretation is presented and discussed.

Keywords: Self-cleaning, wetting, slippery surfaces, contact angle, sliding angle, contact angle hysteresis

1 BACKGROUND

The phenomenon of superhydrophobicity displayed in nature including many plants, insects, and waterfowls has attracted tremendous attention in recent years. A superhydrophobic surface is non-wettable and generally exhibits a very large (static) contact angle ($\theta \geq 150^\circ$), a small sliding angle ($\alpha \sim 10^\circ$ or less) and/or a small contact angle hysteresis. In the case of the

*Corresponding author: E-mail: lawkockyee@gmail.com

Lotus leaf, water droplets usually bead up and roll-off effortlessly. During roll-off, dust particles adhere to the water droplets and are removed from the leaf surface, resulting in the famous self-cleaning effect [1, 2]. In 2008, Roach, Shirtcliffe and Newton [3] pointed out that the above definition of superhydrophobicity is arbitrary, merely representing a consensus number in the literature. On the other hand, Law [4, 5] recently defined superhydrophobicity as a surface having a water advancing angle $\theta_A \geq 145^\circ$ and receding angle $\theta_R > 90^\circ$ by studying the interactive forces of wetting attraction and adhesion between water and 20 different surfaces. As for wettability, a clear measuring scale remains to be defined. Zisman [6] proposed in 1964 that wetting occurs when $\theta = 0^\circ$ and that partially wetting is when $\theta \neq 180^\circ$. Marmur recently suggested to use the contact area between the sessile droplet and the solid surface to measure wettability [7]. In this paper, we loosely define a surface highly wettable when it exhibits a static contact angle of $\sim 50^\circ$ or less with a liquid. Intuitively, a highly wettable surface is not expected to exhibit high liquid droplet mobility due to the small θ value. It is thus very uncommon to have surfaces that are highly wettable and very slippery ($\alpha \leq 10^\circ$) at the same time. Here we report the synthesis and surface properties of surface modified polyurethane coatings that are both highly wettable and slippery. These surfaces also display self-cleaning with hexadecane similar to that observed on the surface of a Lotus leaf. The application of these surfaces in inkjet printing is discussed. The fundamental mechanism that enables both high wettability and slipperiness is put forward and supporting data are presented.

2 EXPERIMENTAL

2.1 Materials

The precursors for the polyurethane coating, the hydroxyl terminated polyacrylate (Desmophen® A870 BA) and hexamethylene diisocyanate (Desmodur® N-3300A) were obtained from Bayer Materials Science. The catalyst for the cross-linking reaction was dibutyl tin dilaurate, RC catalyst 201, from Rhein Chemie. Flow aid (BYK-331) and leveling agent (BYK-358) were obtained from BKY Additives and Instruments. Surface modifying cross-linker Silclean 3700 was obtained from BKY Additives and Instruments and Fluorolink-D was obtained from Solvay Solexis. Methyl isobutyl ketone, n-butyl acetate, methyl n-amyl ketone and methylene chloride were all ACS grade solvents and were purchased from Fisher Scientific. Hexadecane (99.9%) was purchased from Aldrich. Fluorinated solvent FCL-52 was obtained from Cytonix. All solvents were used without further purification. Deionized water (18 M Ω ·cm) was purified by a reverse osmosis process in house. The acrylic based UV ink used in this work was obtained internally.

2.2 Measurements

Contact angle measurements were conducted on an goniometer (OCA20; DataPhysics Instruments, GmbH) from Dataphysics, which consists of a computer-controlled automatic liquid deposition system and a computer-based image processing system. In a typical static contact angle measurement, ~5 μL of the test liquid droplets (water or hexadecane) were gently deposited on the testing surface using a microsyringe and the static contact angle was determined by the computer software (SCA20; DataPhysics Instruments, GmbH) and each reported data is an average of more than 5 independent measurements. Sliding angle measurement was done by tilting the base unit at a rate of $1^\circ/\text{sec}$ with a 10 μL droplet using titling base unit (TBU90E; DataPhysics Instruments, GmbH). All measurements were averaged from 5-8 measurements, using a pristine area of the substrate for each measurement. The tilted angle is defined as the angle where the test liquid droplet starts to slide (or move).

X-ray photoelectron spectroscopy (XPS) was performed on a Kratos instrument using a monochromatic Al X-ray source operated at 280 W and at a pressure of 10^{-9} Torr. The analysis was performed at a takeoff angle of 90° with respect to the sample surface, resulting in an approximate sampling depth of 2-5 nm. XPS data was processing with the CASA-XPS software.

2.3 Preparation of polyurethane based coatings

The base polyurethane coating was prepared by mixing a hydroxyl-terminated polyacrylate (Desmophen® A870 BA in butyl acetate, 70% solids, 28.1 g), hexamethylene diisocyanate (Desmodur® N-3300A, 100% solids, 10.3 g), with 0.29 g of BYK-358, 0.15 g of BYK-331 (10% solids) along with 7 g of n-butyl acetate, 7 g of methyl n-amyl ketone, and 7 g of methyl isobutyl ketone. The mixture was stirred in a beaker along with 0.3 g of a cross-link catalyst, RC catalyst 201 (1% in PMA). The resulting solution was cast onto a Mylar® sheet on a drawbar coater with a 4 mil bar. The coating was first air-dried for ~30 minutes, and then cured at 130°C for about 30 minutes, yielding the base polyurethane coating.

Two types of surface modified coatings were prepared in this work. The first type was prepared by adding varying amount of a polysiloxane crosslinker, Silclean3700 (a hydroxyl functional silicone modified polyacrylate from BYK), to the above polyurethane formulation. The concentration of Silclean 3700 typically varied from 0.5 to 10% by weight relative to the total solid polymer weight of the formulation. The second type of coatings was prepared with cross-linker Fluorolink-D. To ensure thorough mixing between Fluorolink-D and the isocyanate, a fluorinated solvent FCL-52 was used as the coating solvent. The concentration of Fluorolink-D varied from 0.1 to 3% by weight relative to the total solid polymer weight of the formulation. The Fluorolink modified coating was coated and cured as previously described.

3 RESULTS AND DISCUSSION

3.1 Synthesis and Surface Properties of Surface Modified Polyurethane Coatings.

3.1.1 Synthesis

In 2011, we [8] reported the synthesis of surface modified polyurethane coatings by reacting hexamethylene diisocyanate with a hydroxyl-terminated polyacrylate in the presence of surface active cross-linkers, such as SilClean 3700, Fluorolink-D and many of their derivatives. A schematic for the synthesis and the structures of the cross-linkers are given in Figure 1.

3.1.2 Surface properties

Films of the surface modified polyurethanes were obtained by coating the as-synthesized polymer solutions on Mylar substrates. After air drying, the coating was cured at 135°C for 30 min. The surface properties of these films were studied by static contact angle (θ) and sliding angle (α) measurements using the previously described procedures [9]. The data are tabulated in Table 1.

The contact angle data for water and hexadecane as a function of the concentration of the surface active cross-linkers in the polymer coatings are plotted in Figure 2. Static contact angles increase, indicative of increasing hydrophobicity and oleophobicity, as the concentration of the cross-linker increases for both solvents. The elemental content of the coating surface was studied by XPS and the plots for the Si and F signals as a function of the concentration of the surface active cross-linker are given in Figure 3. Both Si and F signals increase rapidly initially and saturate at very low cross-linker concentrations. A visual is provided by the solid lines in Figure 3. More importantly, the increases in Si and F signals

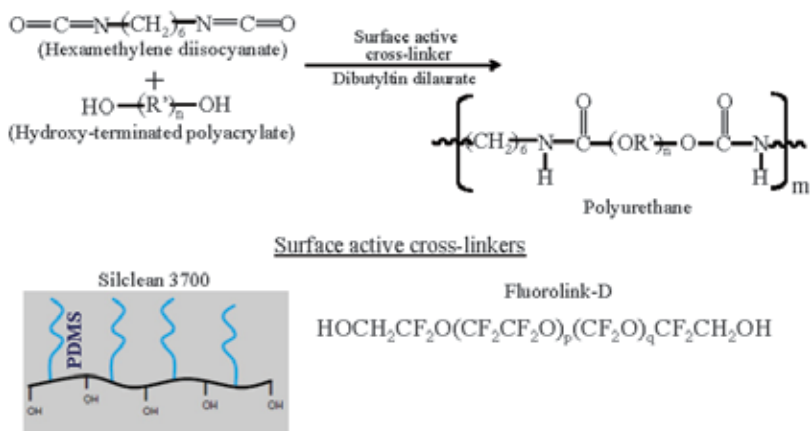


FIGURE 1

Synthesis of polyurethane coatings with surface active cross-linkers.

TABLE 1
Surface properties of polyurethane coatings modified by SilClean 3700 and Fluorolink-D.

% Surface Modifier in PU	Water		Hexadecane	
	θ (°) ^a	α (°) ^b	θ (°) ^a	α (°) ^b
0%	71	52	22	Not measurable ^c
1.9% SilClean	99	31	31	6
3.8% SilClean	102	29	33	4
5.6% SilClean	102	26	33	2
7.5% SilClean	104	23	35	2
0.5% Fluorolink	101	Not slide	64	14
1% Fluorolink	102	63	67	10
1.9% Fluorolink	105	61	67	9
3% Fluorolink	104	63	67	9

a) static contact angle, average of at least 5 measurements, error $<\pm 2^\circ$; b) sliding angle, average of at least 5 measurements, error $<\pm 2^\circ$; c) the hexadecane drop just wet and flow when the surface is tilted.

actually parallel to the increases in the water and hexadecane contact angles, clearly indicating that the low surface energy, surface active functional groups in the cross-linkers locate at the air-surface interface during the film forming step and dominate the surface property of the modified polyurethane coating.

The results in Table 1 also show the impact of the surface active cross-linkers on the sliding angles. The sliding angle is found to decrease as the concentration of the cross-linker increases. The most surprising observations are those with the hexadecane droplets on the SilClean modified coatings. Based on the size of the static contact angles, these surfaces are highly wettable. On the other hand, they all exhibit extremely small sliding angles, $<10^\circ$. For example, for the polyurethane coating modified with 7.5% SilClean 3700, a 2° sliding angle was obtained. Figure 4 depicts the snapshots of the sliding angle data.

3.2 Self-cleaning and applications

Contamination of the surface of inkjet printhead (Figure 5a) has been shown to be the main cause of printer machine being unreliable with high operating cost. Acrylic based UV ink is organic in nature. The slipperiness observed with hexadecane suggests that UV ink may not stick onto the printhead when its surface is coated with the SilClean modified polyurethane coating. Figure 5b shows an offline self-cleaning test involving a polyurethane-SilClean coating on a stainless steel plate (left-hand side). The non-coated side is on the right and is the control. The entire plate was showered with paper dust (white powder) to simulate contamination in the printing environment. When droplets of UV ink

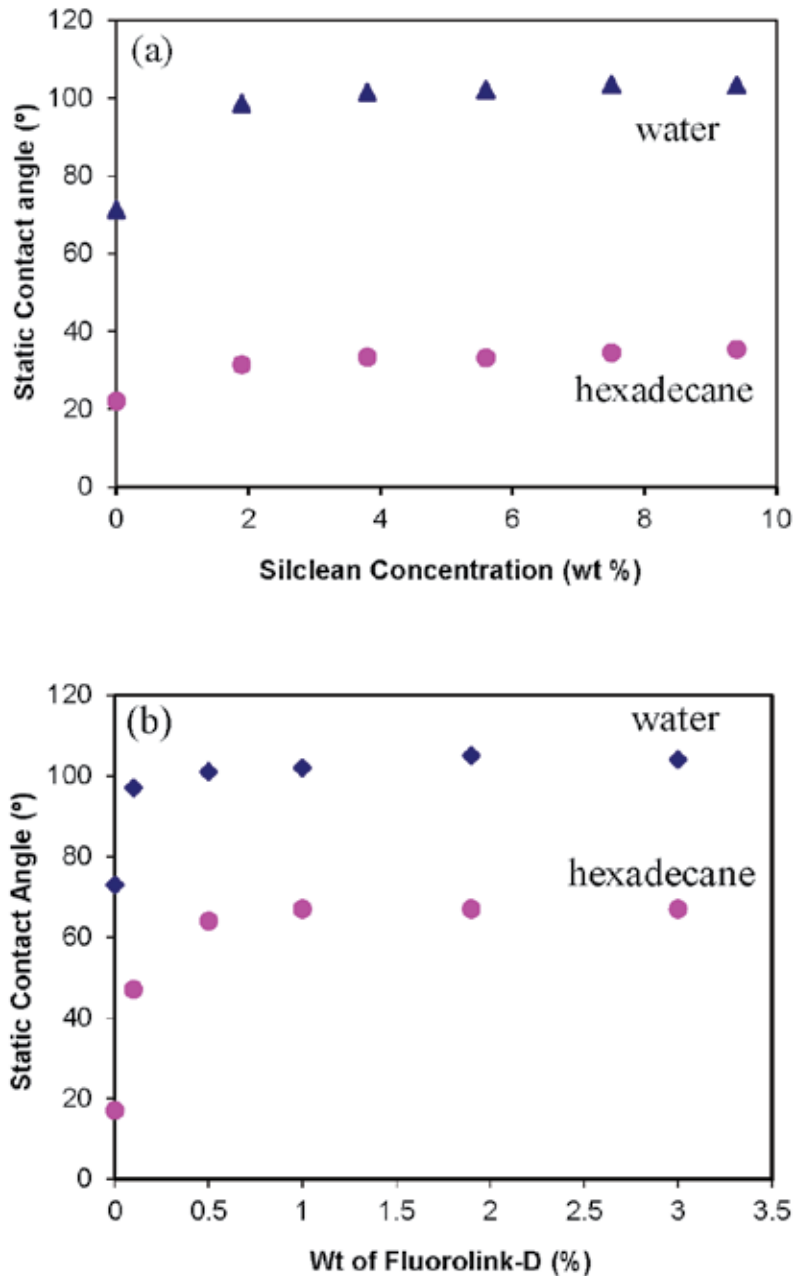


FIGURE 2

Plots of static water and hexadecane contact angles versus surface active cross-linker concentration for (a) SilClean 3700 and (b) Fluorolink-D.

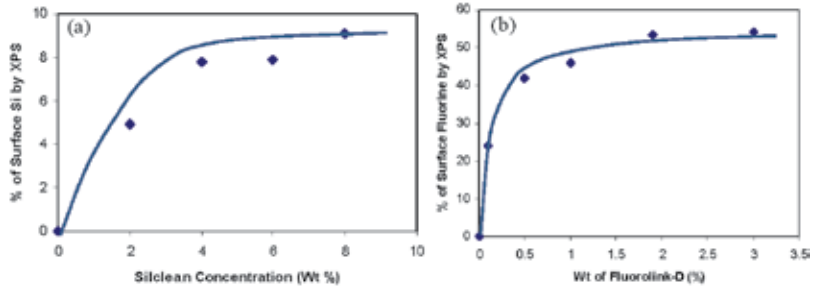


FIGURE 3

Plots of XPS signal as a function of the surface active cross-linker concentration for (a) SilClean 3700 and (b) Fluorolink-D modified polyurethane coatings.

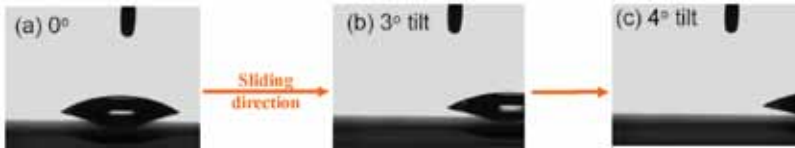


FIGURE 4

Snapshots of the sliding angle data for polyurethane coating modified with 7.5% SilClean 3700.

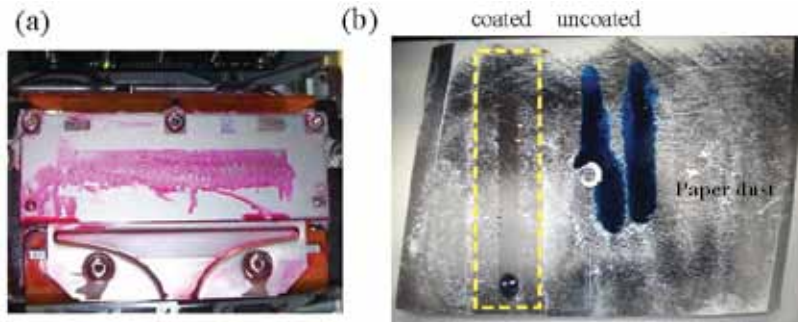


FIGURE 5

(a) Photograph of a contaminated printhead surface and (b) offline UV ink self-cleaning test with a SilClean modified polyurethane coating.

(blue) are dispensed on the surface, paper dust particles are found cleaning off the surface as the ink slides. The cleaning action is similar to that observed on the Lotus leaf. No self-cleaning was observed on the uncoated side. Since the static contact angle for UV ink on the surface is $\sim 40^\circ$, the result demonstrates that self-cleaning is enabled by slipperiness of the surface.

3.3 Mechanism for high wettability with super slipperiness

The interaction between a liquid droplet and the solid surface is expected to be very strong when the liquid is highly wettable. High liquid wettability also

means small θ value. Intuitively, the mobility of the liquid droplet is expected to be low. It is thus very unusual to have surfaces that are highly wettable and very slippery ($\leq 10^\circ$) at the same time. Literature studies however reveal that this phenomenon is not new. For instances, Langmuir and Blodgett [10] observed a completed roll-off of a white mineral oil droplet on a trimolecular stearate Langmuir-Blodgett (LB) film on glass, which exhibited a contact angle of $\sim 55^\circ$. They described the unexpected observation as “de-wetting”, attributable to both the tight packing of the C18 hydrocarbon chain in the LB film as well as the non-interacting nature of the CH_3 end group. In 1996, Schmidt et al. [11] reported the synthesis of a new family of non-sticking, wettable polymers by cross-linking reactive perfluoroalkyl polymeric surfactants with poly(2-isopropenyl-2-oxazoline) at different reactant ratios under various reacting and curing conditions. Static (θ), advancing (θ_A), receding (θ_R) and sliding (α) angles with water and hexadecane were reported. With hexadecane, four of the polymer coatings exhibit static contact angles range between 58° to 67° with sliding angles less than 15° . Recently, surfaces with even smaller static contact angles and sliding angles ($\theta \sim 30\text{-}50^\circ$ and $\alpha < 10^\circ$) have been reported by several research groups: the McCarthy group at University of Massachusetts [12, 13], the Hozumi group at AIST Japan [14-17], the Law group at Xerox [8, 9, 18-21], and the Liu group at Queen’s [22, 23]. All of these surfaces are flat and smooth based on optical microscopy [8] and AFM studies [13-17, 22]. Table 2 highlights typical surface properties observed for some of these surfaces. They are all hydrophobic with water $\theta > 90^\circ$. The most fascinating results are from hexadecane. These surfaces are found to be highly wettable and highly slippery with hexadecane θ ranges between 30° to 70° and sliding angles less than 10° .

Figure 6 shows a schematic of a sliding liquid droplet on an inclined surface. The driving force (F) for the droplet to slide is equal to $mg \cdot \sin\alpha$, where α is the inclination angle, m is the mass of the liquid droplet and g is gravitational constant. The frictional force (f) that keeps the drop from sliding is given by [24, 25]:

$$f = \gamma_{LV} \cdot R \cdot k \cdot (\cos\theta_R - \cos\theta_A), \quad (1)$$

where γ_{LV} is the surface tension of the liquid, R is the length scale for the contour of the drop and k is an adjustable parameter based on experimental data.

At the moment of drop sliding, $F = f$ and α becomes the sliding angle. Krasovitski and Marmur²⁶ equated the sliding angle to θ_A and θ_R as:

$$\sin\alpha = C \cdot \gamma_{LV} \cdot (\cos\theta_R - \cos\theta_A), \quad (2)$$

TABLE 2
Surface Properties of Some Recent Wettable Slippery Surfaces.

Surface	Enabling Functional Group	Liquid	θ^a	θ_A/θ_R^b	$(\theta_A - \theta_R)^c$	α^d	Ref.
1. Alkyl silane from $\text{Cl}(\text{SiMe}_2\text{O})_n\text{SiMe}_2\text{Cl}$ on Si-wafer	PDMS	Water Hexadecane		$\sim 105^\circ/\sim 104^\circ$ $\sim 36^\circ/\sim 35^\circ$	$\sim 1^\circ$ $\sim 1^\circ$	-- --	12
2. Alkyl silane from $(\text{Me}_3\text{SiO})_3\text{SiCH}_2\text{CH}_2\text{Si}(\text{CH}_3)_2\text{Cl}$ on Si-wafer	methylsiloxanes	Water Hexadecane		$\sim 104^\circ/\sim 103^\circ$ $\sim 38^\circ/\sim 36^\circ$	$\sim 1^\circ$ $\sim 2^\circ$	-- --	12
3. Acid catalyzed polymer from $\text{Me}_2\text{Si}(\text{OMe})_2$ on Si-wafer	PDMS like	Water Hexadecane		$\sim 105^\circ/\sim 104^\circ$ $\sim 39^\circ/\sim 38^\circ$	$\sim 1^\circ$ $\sim 1^\circ$	-- --	13
4. Grafted PDMS-20K brush on Si-wafer	PDMS	Water Hexadecane		$\sim 112^\circ/\sim 99^\circ$ $\sim 35^\circ/\sim 30^\circ$	13° 5°	$\sim 1^\circ$ $\sim 4^\circ$	14
5. Perfluorinated polyether terminated brush on Si-wafer	perfluoropolyether	Water Hexadecane	$\sim 119^\circ$ 66°	-- --	-- --	$\sim 19^\circ$ $\sim 8^\circ$	15
6. C10 sol gel hybrid film	$n\text{-C}_{10}\text{H}_{21}$	Water Hexadecane		$\sim 109^\circ/\sim 100^\circ$ $\sim 36^\circ/\sim 34^\circ$	9° 2°	40° 3.4°	16
7. OTS SAM on Si-wafer ^e	$n\text{-C}_{18}\text{H}_{37}$	Water Hexadecane	109° 40°	$117^\circ/95^\circ$ $45^\circ/34^\circ$	22° 11°	13° 8°	9
8. FOTS SAM on Si-wafer ^f	$n\text{-C}_8\text{F}_{17}$	Water Hexadecane	107° 73°	$116^\circ/95^\circ$ $75^\circ/65^\circ$	21° 10°	14° 9°	9
9. Epoxy polymer with copolymerized PDMS group	PDMS	Water Hexadecane	$\sim 100^\circ$ 34°	-- --	-- --	$\sim 40^\circ$ $\sim 3^\circ$	22

(a) θ static contact angle, (b) θ_A advancing contact angle, θ_R receding contact angle, (c) $(\theta_A - \theta_R)$ contact angle hysteresis, (d) α sliding angle, (e) OTS SAM, a self-assembled-monolayer synthesized from octadecyltrichlorosilane; and (f) FOTS SAM, a self-assembled-monolayer synthesized from trideca fluoro-1,1,2,2-tetrahydrooctyltrichlorosilane.

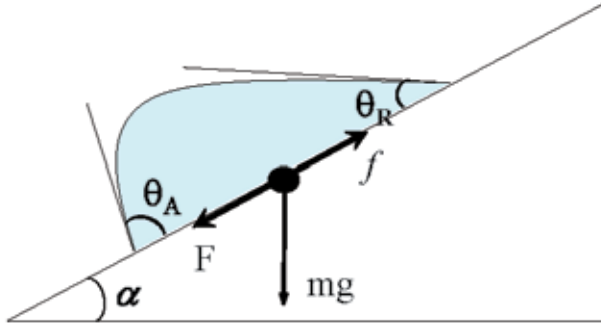


FIGURE 6
Schematic showing different forces acting on a liquid droplet on an inclined surface.

where C is a constant that includes the gravitational acceleration, density of the liquid and the geometric parameters of the drop.

It is clear from Eq(2) that the fundamental driver for having a very small sliding angle (super slipperiness) is when $\theta_A \approx \theta_R$. For a wettable surface, this outcome can be rationalized by a simple thermodynamic consideration. For instance, even though the energy required to de-pin a liquid droplet on a wettable surface is fairly high (small θ_R), it can be well compensated with a favorable wetting interaction (small θ_A) along with a small gain in potential energy through gravity.

One of the remaining questions is why the water droplet is stickier on the same surface despite having a larger water θ ? In other words, with water, θ_A is larger than θ_R , whereas θ_A and θ_R are comparable with hexadecane. This observation can be attributed to the rate of molecular relaxation between liquid molecules and the functional groups at the liquid-solid interface. For example, when water is receding, the contact line always recedes from the wetted area, where water molecules and the functional groups have sufficient time to relax and come to equilibrium at the liquid-solid interface. Contrarily, water molecules and the functional groups may not have enough time to come to equilibrium as the contact line advances to the non-wetted area during advancing. This will result in $\theta_A > \theta_R$. The situation with hexadecane and the slippery surfaces is quite different. The hexadecane solvent molecules and functional groups at the interface, such as PDMS (polydimethylsiloxane) and long alkyl chain, are not only highly compatible, they are also very flexible. Together they facilitate fast molecular relaxation during hexadecane advancing. Consequently, comparable θ_A and θ_R and slippery surfaces result.

Evidence to support the molecular relaxation mechanism comes from data reported by Hozumi et al. [14] in 2012 on a series of PDMS brush grafted surfaces on Si-wafer. The molecular weight (MW) of the PDMS brushes varies from 2,000 to 120,000. The surface properties were studied by advancing

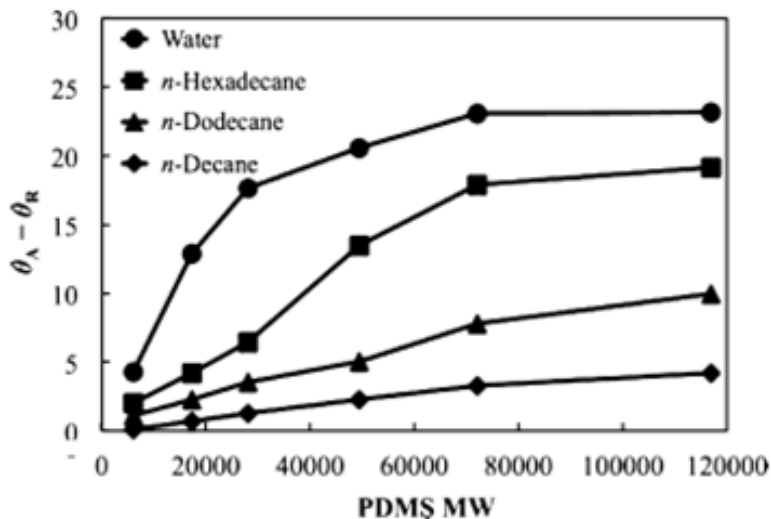


FIGURE 7

Change of $(\theta_A - \theta_R)$ for grafted PDMS surfaces with varying molecular weight. (Reproduced from Ref. 14. Copyright American Chemical Society 2012)

and receding contact angle measurements. Plots of $(\theta_A - \theta_R)$ as a function of the MW of the PDMS brush with water, n-decane, n-dodecane and n-hexadecane are reproduced in Figure 7. Consistent with earlier discussion, $(\theta_A - \theta_R)$ for water is consistently larger than those with hydrocarbon solvents, attributable to the relative incompatibility between water and the PDMS brushes. The significance of the results lies in the PDMS MW effect on the polymer brush and the hydrocarbon chain length effect for the wetting liquid. According to the proposed mechanism, a rapid molecular relaxation between liquid molecules and the PDMS brush at the liquid-solid interface during advancing would lead to $\theta_A = \theta_R$. The data in Figure 7 clearly show that $(\theta_A - \theta_R)$ decreases as the MW of the PDMS brush decreases and as the chain length of the wetting liquid decreases. The results fully support the molecular relaxation mechanism.

Further evidence supporting the mechanism comes from a temperature effect study on the same set of PDMS brush surfaces and the results are summarized in Figure 8. The rate of molecular relaxation is expected to increase as temperature increases. Consistent with the above interpretation, $(\cos\theta_R - \cos\theta_A)$ are shown to be smaller when measured at 70°C as compared to those measured at room temperature for both water and hexadecane.

In polymer chemistry, the compatibility between liquid molecules and polymers are known to correlate to solubility parameter δ [27-29]. To test the hypothesis of the importance of compatibility between liquid and solid

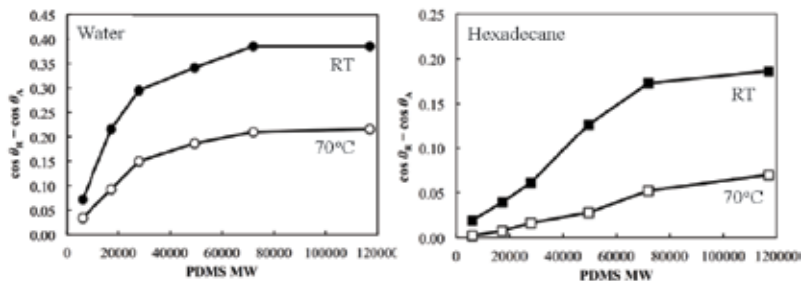


FIGURE 8

Plots of $(\cos\theta_R - \cos\theta_A)$ versus PDMS MW for brush surfaces on Si-wafer with water and hexadecane at 70°C and at room temperature. (Reproduced from Ref. 14. Copyright American Chemical Society 2012)

at the liquid-solid interface, we take the liberty of analyzing several studies in the literature where the effect of solvent on either the contact angle hysteresis and/or sliding angle were investigated. The analysis of the Hozumi study on the C10 hybrid film is given in Figure 9a and those from the McCarthy and Liu studies are given in Figures 9b and 9c, respectively. The correlations are quite good. Consistently, δ increases, indicative of increasing incompatibility, as the contact angle hysteresis or sliding angle increases. These plots again support the molecular relaxation mechanism proposed earlier.

4 CONCLUSIONS

This work shows that the mechanism for super slipperiness on wettable surfaces is a result of their similarity in advancing and receding contact angles. Evidence is provided that fast molecular relaxation between liquid molecules and functional groups at the liquid-solid interface during liquid advancing results in a similar liquid-solid interface between advancing and receding, and $\theta_A \approx \theta_R$. This work also demonstrates that self-cleaning is the result of surface slipperiness or small sliding angle, not the large static contact angle as most publications suggested.

5 ACKNOWLEDGEMENTS

The author thanks Dr. V. Sambhy for his technical contribution and Xerox Corporation for the support during the course of this work. Thanks are also due to Dr. A. Hozumi (AIST Japan) and Professor G. Liu (Queen's University) for data sharing and helpful discussions.

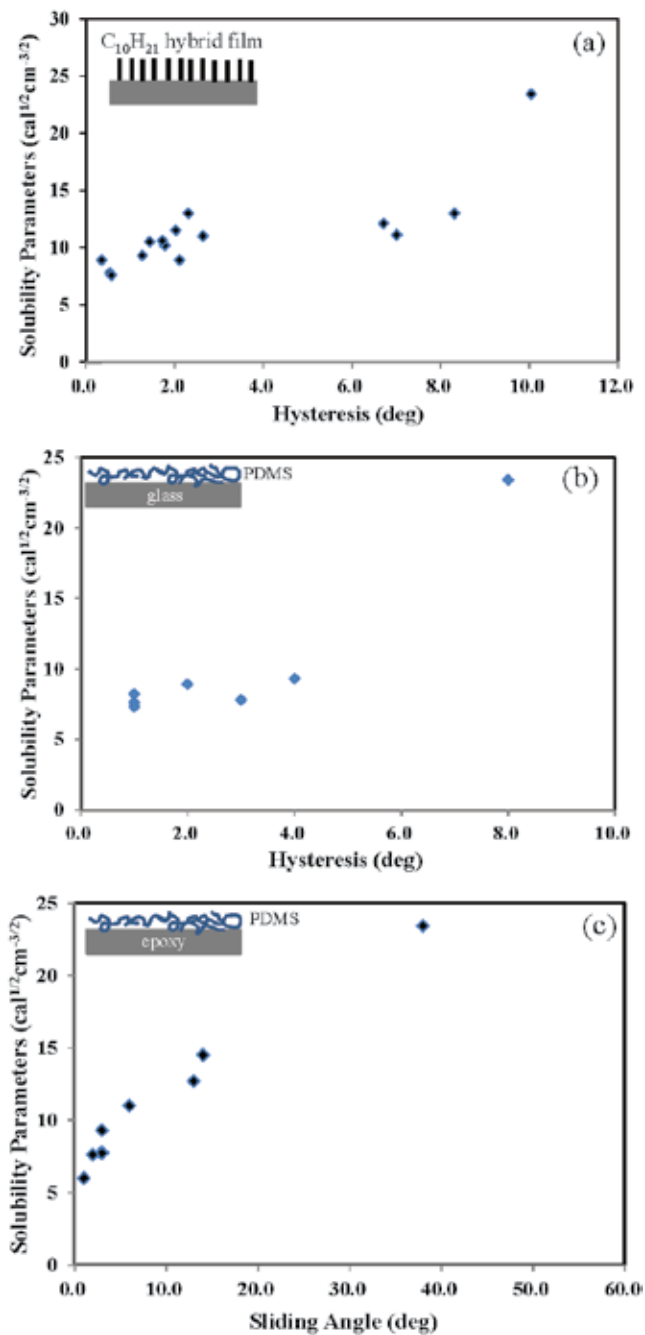


FIGURE 8

Plots of solubility parameter δ versus hysteresis or sliding angle for wettable slippery surfaces shown in the inserts (a. hysteresis data from Ref. 16; b. hysteresis data from Ref. 13, and (c) sliding angle data from Ref. 22)

REFERENCES

- [1] Barthlott W. and Neinhuis C. The purity of sacred lotus or escape from contamination in biological surfaces. *Planta* **202** (1997), 1-8.
- [2] In this work, self-cleaning refers to the cleaning process displayed by the Lotus leaf as reported in Ref. 1. TiO₂ surface also exhibits self-cleaning and is often mentioned in the literature. The self-cleaning mechanism for TiO₂ involves photo-excitation of the semiconductor, followed by the production of the superoxide radical, which oxidizes and cleans any contaminants on the surface.
- [3] Roach P., Shirtcliffe N.J. and Newton, M.I. Progress on superhydrophobic surface development. *Soft Matter* **4** (2008), 224-240.
- [4] Law K.Y. Definitions for hydrophilicity, hydrophobicity, and superhydrophobicity. *The Journal of Physical Chemistry Letters* **5** (2014), 686-688.
- [5] Law K.Y. Water-surface interactions and definitions for hydrophilicity, hydrophobicity, and superhydrophobicity. *Pure and Applied Chemistry* **87** (2015), 759-765.
- [6] Zisman W.A. Relation of the equilibrium contact angle to liquid and solid constitution. In Fowkes F. (Ed) *Contact Angle, Wettability, and Adhesion. Advances in Chemistry*, American Chemical Society, Washington, D.C. 1964, pp. 1-51.
- [7] Marmur A. Superhydrophobic and superhydrophobic surfaces: from understanding non-wettability to design consideration. *Soft Matter* **9** (2013), 7900-7904.
- [8] Law K.Y., Sambhy V. and Zhao, H. (2011) Self-cleaning polymers and coatings. *Proceedings for NSTI Nanotech Conference & Expo*. 13-16 June 2011, Boston MA.
- [9] Zhao H., Law K.Y. and Sambhy V. Fabrication, surface properties, and origin of superoleophobicity for a model textured surface. *Langmuir* **27** (2011), 5927-5935.
- [10] Langmuir I. Mechanical properties of monomolecular films. *Journal of The Franklin Institute* **218** (1934), 143-171.
- [11] Schmidt D.L., DeKoven B.M., Coburn C.E., Potter G.E., Meyers G.F. and Fischer D. A. Characterization of a new family of nonwetttable nonstick surfaces. *Langmuir* **12** (1996), 518-529.
- [12] Chen W., Fadeev A.Y., Hsieh M.C., Oner D., Youngblood J. and McCarthy T.J. Ultrahydrophobic and ultralyophobic surfaces: some comments and examples. *Langmuir* **15** (1999), 3395-3399.
- [13] Wang L. and McCarthy T.J. Covalently attached liquids: instant omniphobic surfaces with unprecedented repellency. *Angewandte Chemie International Edition*, **55** (2016), 244-248.
- [14] Cheng D.F., Urata C., Masheder B. and Hozumi, A. A physical approach to specifically improve the mobility of alkane liquid drops. *Journal of the American Chemical Society*, **134** (2012), 10191-10199.
- [15] Cheng D.F., Masheder B., Urata C. and Hozumi A. Smooth perfluorinated surfaces with different chemical and physical nature: their unusual dynamic dewetting behavior toward polar and non-polar liquids. *Langmuir* **29** (2013), 11322-11329.
- [16] Urata C., Masheder B., Cheng D.F., Miranda D.F., Dunderdale G.J., Miyamae T. and Hozumi A. Why can organic liquids move easily on smooth alkyl-terminated surfaces? *Langmuir* **30** (2014), 4049-4255.
- [17] Urata C., Cheng D.F., Masheder B. and Hozumi, A. Smooth, transparent and non-perfluorinated surfaces exhibiting unusual contact angle behavior towards organic liquids. *RSC Advances* **2** (2012), 9805-9808.
- [18] Kovacs G.J., Law K.Y., Zhao H. and Sambhy V. *Coating for an Ink Jet Printhead Front Face*. U.S. Patent 8226207, 24th July 2012.
- [19] Sambhy V., Law K.Y., Zhao H. and Chugh S. *Thermally Stable Oleophobic Low Adhesion Coating for Inkjet Printhead Front Face*. U.S. Patent 8544987, 1st October 2013.
- [20] Sambhy V., Law K.Y., Zhao H. and Chugh, S. *Low Adhesion Sol Gel Coatings with High Thermal Stability for Easy Clean, Self-Cleaning Printhead Front Face Applications*. U.S. Patent 8851630, 7th October 2014.

- [21] Sambhy V., Law K.Y., Zhao H., Gulvin P.M. and Casella, J. M. *Improved Process for Thermally Stable Oleophobic Low Adhesion Coating for Inkjet Printhead Front Face*. U.S. Patent 9073323, 7th July 2015.
- [22] Hu H., Liu G. and Wang, J. Clear and durable epoxy coatings that exhibit dynamic omniphobicity. *Advanced Materials Interfaces*. **3** (2016), 1600001.
- [23] Rabnawaz M., Liu G. and Hu H. Graft-copolymer based approach to clear, durable, and anti-smudge polyurethane coatings. *Angewandte Chemie International Edition*. **54** (2015), 6516-6520.
- [24] Macdougall G. and Ockrent C. Surface energy relations in liquid/solid systems. 1. The adhesion of liquids to solids and a new method of determining the surface tension of liquids. *Proceedings of the Royal Society of London A*. **180** (1942), 151-173.
- [25] Furnidge G.C.L. Studies at phase interfaces i. The sliding of liquid drops on solid surfaces and a theory for spray retention. *Journal of Colloid Science*. **17** (1962), 309-324.
- [26] Krasovitski B. and Marmur, A. Drops down the hill: theoretical study of limiting contact angles and the hysteresis range on a tilted plate. *Langmuir* **21** (2005), 3881-3885.
- [27] Hansen C.M. and Smith, A.L. Using hansen solubility parameters to correlate solubility of c60 fullerene in organic solvents and in polymers. *Carbon* **42** (2004), 1591-1597.
- [28] Hansen, C.M. 50 Years with solubility parameters – past and future. *Progress in Organic Coatings* **51** (2004), 77-84.
- [29] Hansen C.M. *Hansen Solubility Parameters: A User's Handbook*, 2nd edition, Boca Baton, FL: CRC Press. 2007